Circuits Syst Signal Process (2016) 35:163–184
DOI 10.1007/s00034-015-0048-y

Waveform Optimization for Target Scattering Coefficients Estimation Under Detection and Peak-to-Average Power Ratio Constraints in Cognitive Radar

Peng Chen[1] · **Lenan Wu**[1] · **Chenhao Qi**[1]

Received: 14 July 2014 / Revised: 30 March 2015 / Accepted: 1 April 2015 /
Published online: 17 April 2015
© Springer Science+Business Media New York 2015

Abstract This work investigates the estimation of target scattering coefficients (TSC) in cognitive radar systems with temporally correlated targets. An estimation method based on Kalman filtering (KF) is proposed to exploit the temporal TSC correlation between the pulses in the frequency domain. To minimize the mean square error of the estimated TSC at each KF iteration, unlike existing indirect methods, in this paper the radar waveform is optimized directly under the constraints of transmitted power, peak-to-average power ratio (PAPR) and detection probability. Since the optimization problem regarding the waveform design is non-convex, a novel method is proposed to convert this problem into a convex one. Simulation results demonstrate that the performance of the TSC estimation for the temporally correlated target is significantly improved by radar waveform optimization. Meanwhile, no performance degradation is observed with the introduction of the additional PAPR constraints and the detection constraints for KF estimation with the optimized waveform.

Keywords Cognitive radar system · Detection probability · Kalman filtering · PAPR · Radar waveform optimization

✉ Chenhao Qi
qch@seu.edu.cn

Peng Chen
chenpengdsp@seu.edu.cn

Lenan Wu
wuln@seu.edu.cn

[1] School of Information Science and Engineering, Southeast University, Nanjing 210096, China

1 Introduction

In cognitive radar systems (CRS), the transmitted waveform can be designed in such a way that it adapts to the environments and characteristics of the targets, which thus improves the overall target detection and recognition performance [9]. The extended target in CRS, which can occupy more than one resolution cell, is often described using either the target impulse response (TIR) in the time domain [1] or the target scattering coefficients (TSC) in the frequency domain [27]. The estimation performance of the TSC or the TIR can be improved by optimizing the transmitted waveform [28]. In general, there are two popular criteria for waveform optimization [1,5,16]. One is based on the signal-to-noise ratio (SNR) or the signal-to-interference-and-noise ratio (SINR) of the echo signal. The other is based on the mutual information shared between the echo signal and the TSC. In practice, many different constraints must also be considered during the waveform optimization, including the constraints for the range and velocity resolutions and the constraint of constant envelope considering the efficiency of the nonlinear power amplifier [15,18]. However, in the existing works on waveform design for temporally correlated targets, only indirect methods based on water filling have been proposed.

Generally, there are three methods to model the extended target, including

1. Modeling of the extended target as a determinant TIR function, which remains constant during the waveform design [6,7];
2. Modeling of the extended target as a random process with an unknown distribution [1];
3. Modeling of the extended target as a random process with a known distribution, e.g., the Swerling I or Gaussian distribution [16,19,22].

However, considering the fact that the slow change of the angle in the target view leads to the TSC temporal correlation during each pulse repetition interval (PRI) [3], a more appropriate model based on wide sense stationary-uncorrelated scattering (WSSUS) has been proposed [4,29] to describe the extended target. This type of extended target is named in short as a temporally correlated target in this work.

In the study of CRS, increasing attention is being paid to radar waveform design with a constant envelope, and many methods have been proposed [13,14,25]. For example, an orthogonal frequency division multiplexing (OFDM) signal with a constant envelope was optimized in [12,24]. Because this constant envelope constraint is too strict, the peak-to-average power ratio (PAPR) can be used as a relaxed form [17,20–22]. In the same context, radar waveform design under the PAPR constraint has been considered in [22]. However, waveform design for a temporally correlated target has not been investigated thoroughly. Even if the radar systems cannot provide precise estimation of the TSC, the binary detection in terms of presence or absence of the target is still needed. Thus, the detection ability is essential during the waveform optimization [11,26].

In this work, an estimation method based on Kalman filtering (KF) in the frequency domain is proposed to exploit the temporal correlation of the TSC. Moreover, to minimize the mean square error (MSE) of the estimated TSC at each KF iteration, unlike existing indirect methods, the radar waveform is optimized directly by the proposed

method under the constraints of the transmitted power, the PAPR and the detection probability. Since the waveform optimization problem is non-convex, a novel method is proposed to solve it by converting the existing non-convex problem into a convex one.

This manuscript is organized as follows. In Sect. 2, the radar system with the temporally correlated target is described. The TSC estimation method based on KF is proposed. In Sect. 3, optimization of the radar waveform under the constraints of the transmitted power, the PAPR and the target detection probability is presented. Simulation results are given in Sect. 4, and finally Sect. 5 concludes this work.

The notations used in this work are defined as follows. Symbols for vectors (lower case) and matrices (upper case) are in bold face. I, $\mathcal{N}(0, \mathbf{R})$, $(\cdot)^H$, $\mathrm{diag}\{\cdot\}$, $\mathcal{E}\{\cdot\}$, $\mathbf{F}$, $\|\cdot\|_2$, $\mathrm{Re}\{\cdot\}$ and $\mathrm{Tr}\{\cdot\}$ denote the identity matrices, the Gaussian distribution with zero mean and covariance of $\mathbf{R}$, the conjugate transpose (Hermitian), the diagonal matrix, the expectation, the Fourier transform, the ℓ_2 norm, and the real part and the trace of a matrix, respectively.

2 Cognitive Radar System and TSC Estimation Based on KF

The CRS with the temporally correlated target that is considered in this work is shown in Fig. 1, where the echo signal $\mathbf{r}_k$ during the kth pulse includes the additive colored Gaussian noise $\mathbf{n}_k \sim \mathcal{N}\left(\mathbf{0}, \mathbf{R}'_N\right)$ with zero mean and covariance matrix being $\mathbf{R}'_N$. In the presence of a target, the echo signal can be modeled as

$$\mathbf{r}_k = \mathbf{H}_k \mathbf{s}_k + \mathbf{n}_k, \tag{1}$$

where $\mathbf{s}_k \in \mathbb{R}^{M\times 1}$ denotes the transmitted radar waveform during the kth pulse, and $\mathbf{H}_k$ denotes the convolution matrix of the TIR $\mathbf{h}_k$, which can be written as

$$\mathbf{H}_k = \begin{pmatrix} h_{k,1} & h_{k,M} & \dots & h_{k,2} \\ h_{k,2} & h_{k,1} & \dots & h_{k,3} \\ \vdots & \vdots & \ddots & \vdots \\ h_{k,M-1} & h_{k,M-2} & \dots & h_{k,M} \\ h_{k,M} & h_{k,M-1} & \dots & h_{k,1} \end{pmatrix}, \tag{2}$$

where $h_{k,m}(m = 1, \dots, M)$ denotes the mth entry of the TIR $\mathbf{h}_k$.

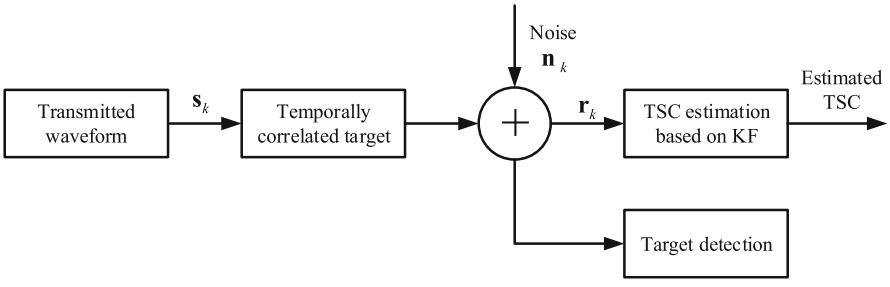

Fig. 1 CRS with temporally correlated target

Because a relative change in the viewing angle between the target and the radar causes the fluctuation in the TIR, the WSSUS model can be used to describe this fluctuation. Therefore, the TIR $\mathbf{h}_k$ during the kth pulse can be represented as

$$\mathbf{h}_k = e^{-T/\tau}\mathbf{h}_{k-1} + \mathbf{u}_{k-1}, \tag{3}$$

where $\mathbf{u}_{k-1} \sim \mathcal{N}\left(\mathbf{0}, \left(1 - e^{-2T/\tau}\right)\mathbf{R}'_T\right)$ denotes the zero mean Gaussian vector, which describes the TIR fluctuation [3,4,29]. $\mathbf{R}'_T$, $\mathbf{T}$ and τ denote, respectively, the covariance matrix of the TIR $\mathbf{h}_k$, the PRI and a constant that describes the temporal correlation of the TIR during the PRI.

Then, the echo signal in the frequency domain is

$$\mathbf{y}_k = \mathbf{F}\mathbf{r}_k = \mathbf{Z}_k\mathbf{g}_k + \mathbf{w}_k, \tag{4}$$

where $\mathbf{F}$ denotes the Fourier transform matrix, $\mathbf{w}_k \sim \mathcal{N}\left(\mathbf{0}, \mathbf{R}_N \triangleq \mathbf{F}\mathbf{R}'_N\mathbf{F}\right)$ denotes the additive Gaussian noise in the frequency domain, $\mathbf{z}_k \triangleq \mathbf{F}\mathbf{s}_k$, $\mathbf{Z}_k \triangleq \mathrm{diag}\{\mathbf{z}\}$ is a diagonal matrix of the radar waveform in the frequency domain, and $\mathbf{g}_k \triangleq \mathbf{F}\mathbf{h}_k$, with $\mathbf{g}_k \sim \mathcal{N}(\mathbf{0}, \mathbf{R}_T)$.

With its knowledge of both the target and the environment, the CRS can provide better target detection and classification performance than traditional radar systems. First, we will give an estimation algorithm based on the maximum a posteriori probability (MAP).

In the presence of a target, we have $\mathbf{y}_k \sim \mathcal{N}(\mathbf{0}, \mathbf{R}_k)$, where

$$\begin{aligned}\mathbf{R}_k &\triangleq \mathcal{E}\left\{\left(\mathbf{Z}_k\mathbf{g}_k + \mathbf{w}_k\right)\left(\mathbf{Z}_k\mathbf{g}_k + \mathbf{w}_k\right)^H\right\} \\ &= \mathbf{Z}_k\mathbf{R}_T\mathbf{Z}_k^H + \mathbf{R}_N.\end{aligned} \tag{5}$$

In the absence of a target, we have $\mathbf{y}_k \sim \mathcal{N}(\mathbf{0}, \mathbf{R}_N)$. Therefore, the TSC estimation algorithm based on MAP can be expressed as

$$\hat{\mathbf{g}}_k = \arg\max_{\mathbf{g}_k} \; p\left(\mathbf{g}_k \,|\, \mathbf{y}_k\right). \tag{6}$$

From (4) to (6), we can obtain the estimated TSC (with the details provided in Appendix 1) as

$$\hat{\mathbf{g}}_k = \arg\min_{\mathbf{g}_k} \; \left\{\mathbf{g}_k^H\left(\mathbf{Z}_k^H\mathbf{R}_N^{-1}\mathbf{Z}_k + \mathbf{R}_T^{-1}\right)\mathbf{g}_k - \mathbf{y}_k^H\mathbf{R}_N^{-1}\mathbf{Z}_k\mathbf{g}_k - \mathbf{g}_k^H\mathbf{Z}_k^H\mathbf{R}_N^{-1}\mathbf{y}_k\right\}. \tag{7}$$

Algorithm 1 TSC estimation based on the KF

1: Set the iteration index to $k = 2$, where the maximum number of iterations is $K_{\max}$. The MAP method is used to estimate the TSC

$$\hat{\mathbf{g}}_{1|1} = \mathbf{Q}_1 \mathbf{y}_1, \tag{8}$$

and the initial MSE matrix of the estimated TSC is

$$p_{1|1} = \mathcal{E}\left\{ (\mathbf{Q}_1 \mathbf{y}_1 - \mathbf{g}_1)(\mathbf{Q}_1 \mathbf{y}_1 - \mathbf{g}_1)^H \right\} \tag{9}$$

$$= \mathbf{Q}_1 \left(\mathbf{Z}_1 \mathbf{R}_1 \mathbf{Z}_1^H + \mathbf{R}_N \right) \mathbf{Q}_1^H - \mathbf{Q}_1 \mathbf{Z}_1 \mathbf{R}_T - \mathbf{R}_T \mathbf{Z}_1^H \mathbf{Q}_1^H + \mathbf{R}_T,$$

where $\mathbf{Q}_1$ is the MAP filtering matrix;

2: **while** $k \leq K_{\max}$ **do**

3: Because of the temporal correlation of TSC, we can obtain the TSC prediction from (3):

$$\hat{\mathbf{g}}_{k|k-1} = e^{-T/\tau} \hat{\mathbf{g}}_{k-1|k-1}; \tag{10}$$

4: Based on the predicted TSC, the estimated MSE matrix is

$$\mathbf{P}_{k|k-1} = e^{-2T/\tau} \mathbf{P}_{k-1|k-1} + \left(1 - e^{-2T/\tau} \right) \mathbf{R}_T; \tag{11}$$

5: We define the Kalman gain matrix as

$$\mathbf{\Phi}_k \triangleq \mathbf{P}_{k|k-1} \mathbf{Z}_k^H \left(\mathbf{Q}_k \mathbf{R}_N + \mathbf{Q}_k \mathbf{Z}_k \mathbf{P}_{k|k-1} \mathbf{Z}_k^H \right)^{-1}; \tag{12}$$

6: The estimated TSC are then

$$\hat{\mathbf{g}}_{k|k} = \hat{\mathbf{g}}_{k|k-1} + \mathbf{\Phi}_k \left(\hat{\mathbf{g}}_k - \mathbf{Q}_k \mathbf{Z}_k \hat{\mathbf{g}}_{k|k-1} \right) \tag{13}$$

where $\hat{\mathbf{g}}_k = \mathbf{Q} \mathbf{y}_k$;

7: The MSE matrix is

$$\mathbf{P}_{k|k} = \mathbf{P}_{k|k-1} - \mathbf{\Phi}_k \mathbf{Q}_k \mathbf{Z}_k \mathbf{P}_{k|k-1}; \tag{14}$$

8: Let $k = k + 1$;

9: **end while**

Then, the estimated TSC based on the MAP are

$$\hat{\mathbf{g}}_k = \left(\mathbf{Z}_k^H \mathbf{R}_N^{-1} \mathbf{Z}_k + \mathbf{R}_T^{-1} \right)^{-1} \mathbf{Z}_k^H \mathbf{R}_N^{-1} \mathbf{y}_k, \tag{15}$$

and the MAP filtering matrix is

$$\mathbf{Q}_k = \left(\mathbf{Z}_k^H \mathbf{R}_N^{-1} \mathbf{Z}_k + \mathbf{R}_T^{-1} \right)^{-1} \mathbf{Z}_k^H \mathbf{R}_N^{-1}. \tag{16}$$

The MSE of the MAP estimation is

$$e_{\mathrm{MAP}} = \mathcal{E}\left\{\left\|\hat{\mathbf{g}}_k - \mathbf{g}_k\right\|_2^2\right\} \tag{17}$$
$$= \mathrm{Tr}\left\{\mathbf{Q}_k^H\mathbf{Q}_k\left(\mathbf{Z}_k\mathbf{g}_k\mathbf{g}_k^H\mathbf{Z}_k^H + \mathbf{R}_N\right) - \mathbf{g}_k^H\left(\mathbf{Z}_k^H\mathbf{Q}_k^H + \mathbf{Q}_k\mathbf{Z}_k - I\right)\mathbf{g}_k\right\}.$$

In this work, a TSC estimation method based on KF with MAP estimation is proposed to take advantage of the TIR temporal correlation. The prediction and the estimation are combined to improve the estimation performance. The details are given in Algorithm 1.

3 Waveform Optimization Under Detection and PAPR Constraints

To ensure the efficiency of the nonlinear power amplifier, the power amplifier must operate in the linear region. Therefore, the PAPR of the transmitted signal must be below a certain threshold. In addition, the radar systems must be able to detect the target when the estimated TSC cannot be obtained accurately. After consideration of these two factors, we optimize the radar waveform to minimize the MSE of the estimated TSC at each KF iteration step under the constraints of PAPR and detection probability. This optimization problem can be described as

$$\begin{aligned}\mathbf{s}_k^* = \arg\min_{\mathbf{s}_k}\ & \left\{f\left(\mathbf{z}_k\right) \triangleq \mathrm{Tr}\left\{\mathbf{P}_{k|k}\right\}\right\} \\ \text{s.t. }\ & \|\mathbf{s}_k\|_2^2 = E_s \\ & \mathrm{PAPR}\left(\mathbf{s}_k\right) \le \zeta \\ & P_D\left(P_{\mathrm{FA}}\right) \ge \epsilon \\ & \mathbf{z}_k = \mathbf{F}\mathbf{s}_k,\end{aligned} \tag{18}$$

where $\|\mathbf{s}_k\|_2^2 = E_s$ is the constraint for transmitted power, $\mathrm{PAPR}\left(\mathbf{s}_k\right) \le \zeta$ is the constraint for PAPR, and $P_D\left(P_{\mathrm{FA}}\right) \ge \epsilon$ is the constraint for the detection probability with the false alarm rate P_{FA}. The objective function is the MSE of the estimated TSC based on the KF, which can be simplified as follows

$$\begin{aligned}\mathbf{P}_{k|k} &= \mathbf{P}_{k|k-1} - \mathbf{P}_{k|k-1}\mathbf{Z}^H\mathbf{Q}^H\left(\mathbf{Q}\mathbf{R}_N\mathbf{Q}^H + \mathbf{Q}\mathbf{Z}\mathbf{P}_{k|k-1}\mathbf{Z}^H\mathbf{Q}^H\right)^{-1}\mathbf{Q}\mathbf{Z}\mathbf{P}_{k|k-1} \\ &= \left(\mathbf{P}_{k|k-1}^{-1} + \mathbf{Z}^H\mathbf{R}_N^{-1}\mathbf{Z}\right)^{-1},\end{aligned} \tag{19}$$

where the Woodbury identity[1] is adopted in the matrix calculation above.

[1] $\left(\mathbf{A}+\mathbf{C}\mathbf{B}\mathbf{C}^H\right)^{-1} = \mathbf{A}^{-1} - \mathbf{A}^{-1}\mathbf{C}\left(\mathbf{B}^{-1} + \mathbf{C}^H\mathbf{A}^{-1}\mathbf{C}\right)^{-1}\mathbf{C}^H\mathbf{A}^{-1}$.

3.1 Simplification of the Optimization Problem

To solve the optimization problem of (18), we must first simplify the constraints. The PAPR is defined as

$$\mathrm{PAPR}\left(\mathbf{s}_k\right) \triangleq 10\log_{10}\left(M\frac{\max_{1\le m\le M}\left|s_{k,m}\right|^2}{\mathbf{s}_k^H\mathbf{s}_k}\right), \tag{20}$$

where $s_{k,m}$ denotes the mth entry of $\mathbf{s}_k$. The PAPR constraint can then be rewritten as

$$\max_{1\le m\le M}\left|s_{k,m}\right|^2 \le \frac{10^{\zeta/10}}{M}\mathbf{s}_k^H\mathbf{s}_k = \frac{10^{\zeta/10}}{M}E_s \triangleq \zeta' E_s. \tag{21}$$

The constraint for target detection is simplified as follows. During the target detection, the detection performance can be improved significantly by the knowledge of the TSC. However, the TSC are unknown, and thus an estimate of the TSC based on the KF is needed to design the radar waveform and subsequently to detect the target. If we assume that H_1 and H_0 represent the presence and the absence of the target, respectively, then the distributions of the echo signals are

$$\mathbf{y}_k|\,H_0 \sim \mathcal{N}\left(\mathbf{0},\mathbf{R}_N\right) \tag{22}$$

$$\mathbf{y}_k|\,H_1 \sim \mathcal{N}\left(\mathbf{Z}\hat{\mathbf{g}}_k,\mathbf{R}_N\right), \tag{23}$$

where $\hat{\mathbf{g}}_k$ are the estimated TSC based on the KF. Then the target detection likelihood ratio is:

$$\begin{aligned} l'\left(\mathbf{y}_k\right) &= \frac{\mathcal{N}\left(\mathbf{Z}_k\hat{\mathbf{g}}_k,\mathbf{R}_N\right)}{\mathcal{N}\left(\mathbf{0},\mathbf{R}_N\right)} \underset{H_0}{\overset{H_1}{\gtrless}} \theta' \\ \Rightarrow l\left(\mathbf{y}_k\right) &= \mathbf{y}_k^H\mathbf{R}_N^{-1}\left(\mathbf{Z}_k\hat{\mathbf{g}}_k\right) \underset{H_0}{\overset{H_1}{\gtrless}} \theta, \end{aligned} \tag{24}$$

where θ denotes the detection threshold. The false alarm rate based on the constant false alarm rate (CFAR) is given by

$$\begin{aligned} P_{\mathrm{FA}} &= P\left(\mathbf{w}_k^H\mathbf{R}_N^{-1}\left(\mathbf{Z}_k\hat{\mathbf{g}}_k\right) \ge \theta\right) \\ &= Q\left(\frac{\theta}{\sqrt{\left(\mathbf{Z}_k\hat{\mathbf{g}}_k\right)^H\mathbf{R}_N^{-1}\left(\mathbf{Z}_k\hat{\mathbf{g}}_k\right)}}\right), \end{aligned} \tag{25}$$

where $Q\left(x\right) = \frac{1}{\sqrt{2\pi}}\int_x^\infty \exp\left(-\frac{\mu^2}{2}\right)\mathrm{d}\mu$ is the Q-function. The detection threshold in (24) is

$$\theta\left(P_{\mathrm{FA}}\right) = Q^{-1}\left(P_{\mathrm{FA}}\right)\sqrt{\left(\mathbf{Z}\hat{\mathbf{g}}_k\right)^H\mathbf{R}_N^{-1}\left(\mathbf{Z}\hat{\mathbf{g}}_k\right)}. \tag{26}$$

The target detection probability can then be obtained as

$$P_D\left(P_{\mathrm{FA}}\right) = Q\left(Q^{-1}\left(P_{\mathrm{FA}}\right) - \sqrt{\left(\mathbf{Z}_k\hat{\mathbf{g}}_k\right)^H \mathbf{R}_N^{-1}\left(\mathbf{Z}_k\hat{\mathbf{g}}_k\right)}\right). \tag{27}$$

With a sufficiently large number of KF iterations, the estimated TSC will approach the real TSC, i.e., $\mathbf{g}_k \approx \hat{\mathbf{g}}_k$. Since $Q(x)$ is a monotonically decreasing function of x, the constraint $P_D\left(P_{\mathrm{FA}}\right) \geq \epsilon$ can then be written as

$$p\left(\mathbf{z}_k\right) \triangleq \mathbf{z}_k^H \hat{\mathbf{G}}_k^H \mathbf{R}_N^{-1} \hat{\mathbf{G}}_k \mathbf{z}_k \geq \epsilon', \tag{28}$$

where $\hat{\mathbf{G}}_k \triangleq \mathrm{diag}\left\{\hat{\mathbf{g}}_k\right\}$. This optimization problem is non-convex, where the optimum radar waveform cannot be directly obtained. Therefore, we now propose a method to minimize the MSE of the estimated TSC for each KF iteration. Let

$$\mathbf{T}_k \triangleq \mathbf{V}_k \circ \mathbf{R}_N^{-1}, \tag{29}$$

where $\circ$ denotes the Hadamard product, and $\mathbf{V}_k \triangleq \left(\mathbf{z}_k\mathbf{z}_k^H\right)^T$. Then the objective function $f\left(\mathbf{z}_k\right)$ from (18) is

$$f\left(\mathbf{z}_k\right) = \mathrm{Tr}\left\{\left(\mathbf{P}_{k|k-1}^{-1} + \mathbf{V}_k \circ \mathbf{R}_N^{-1}\right)^{-1}\right\}. \tag{30}$$

Finally, (18) can be written as

$$\begin{aligned} \mathbf{z}_k^* = \arg\min_{\mathbf{z}_k} \ & \mathrm{Tr}\left\{\left(\mathbf{P}_{k|k-1}^{-1} + \mathbf{V}_k \circ \mathbf{R}_N^{-1}\right)^{-1}\right\} \\ \text{s.t. } & \mathbf{z}_k^H \mathbf{z} = E_s \\ & \sqrt{\zeta' E_s I} - \mathrm{diag}\left\{\mathbf{F}^{-1}\mathbf{z}_k\right\} \succeq 0 \\ & \sqrt{\zeta' E_s I} + \mathrm{diag}\left\{\mathbf{F}^{-1}\mathbf{z}_k\right\} \succeq 0 \\ & p\left(\mathbf{z}_k\right) \geq \epsilon', \end{aligned} \tag{31}$$

where $\mathbf{A} \succeq 0$ indicates that $\mathbf{A}$ is a semidefinite matrix. The target detection constraint is described by the function $p\left(\mathbf{z}_k\right)$, which can achieve a maximum value via eigen-decomposition [23]. When $\mathbf{z}_k$ is the eigenvector corresponding to the maximum eigenvalue of the matrix $\mathbf{L}_k \triangleq \hat{\mathbf{G}}_k^H \mathbf{R}_N^{-1} \hat{\mathbf{G}}_k$, we have the maximum value of $p\left(\mathbf{z}_k\right)$ as

$$\lambda_{\max}\mathbf{v}_{\max}^H\mathbf{v}_{\max} = \lambda_{\max}E_s = \max_{\mathbf{z}_k}\ p\left(\mathbf{z}_k\right), \tag{32}$$

where $\lambda_{\max}$ is the maximum eigenvalue of $\mathbf{L}_k$ and $\mathbf{v}_{\max}$ is the corresponding maximum eigenvector. Therefore, $\lambda_{\max}\mathbf{v}_{\max}^H\mathbf{v}_{\max} \geq \epsilon'$ is a necessary condition for the optimization problem in (31).

3.2 Solution of the Optimization Problem

In this subsection, we will solve the optimization problem given by (31). Because this problem cannot be directly solved, we will discuss in two cases. In the first case, we do not consider the PAPR constraint, which is equivalently to assume that both $\mathbf{P}_{k|k-1}$ and $\mathbf{R}_N$ are diagonal matrices. We can simplify the optimization problem in (31) and lead it to be a convex problem, where an analytical expression can be derived. In the second case, we take the PAPR constraint into account, and (31) is non-convex. Then we propose a novel method to convert it into a convex problem.

If we do not consider the PAPR constraint, which is equivalently to assume that both $\mathbf{P}_{k|k-1}$ and $\mathbf{R}_N$ are diagonal matrices, we can rewrite the optimization problem in (31) as

$$\begin{aligned}\mathbf{z}^* = \arg\min_{\mathbf{z}_k} & \sum_{m=1}^{M} \frac{P_{k|k-1,m} R_{N,m}}{R_{N,m} + z_{k,m}^H z_{k,m} P_{k|k-1,m}} \\ \text{s.t. } & \mathbf{z}_k^H \mathbf{z}_k = E_s \\ & \sqrt{\zeta' E_s I} - \operatorname{diag}\left\{\mathbf{F}^{-1}\mathbf{z}_k\right\} \succeq 0 \\ & \sqrt{\zeta' E_s I} + \operatorname{diag}\left\{\mathbf{F}^{-1}\mathbf{z}_k\right\} \succeq 0 \\ & p\left(\mathbf{z}_k\right) \geq \epsilon',\end{aligned} \tag{33}$$

where $z_{k,m}$ denotes the mth entry of $\mathbf{z}_k$ and $P_{k|k-1,m}$ and $R_{N,m}$ denote the mth row and mth column of $\mathbf{P}_{k|k-1}$ and $\mathbf{R}_N$, respectively.

To solve the optimization problem in (33), we use the Lagrange function as

$$\begin{aligned}g\left(\mathbf{z}_k, \lambda_1, \lambda_2\right) \triangleq & \sum_{m=1}^{M} \frac{P_{k|k-1,m} R_{N,m}}{R_{N,m} + z_{k,m}^H z_{k,m} P_{k|k-1,m}} + \lambda_1 \left(p\left(\mathbf{z}_k\right) - \epsilon'\right) \\ & + \lambda_2 \left(\mathbf{z}_k^H \mathbf{z}_k - E_s\right).\end{aligned} \tag{34}$$

The extreme value of (34) can be attained using

$$\frac{\partial g\left(\mathbf{z}, \lambda_1, \lambda_2\right)}{\partial \left\|z_m\right\|_2^2} = 0, \tag{35}$$

where

$$\frac{\partial g\left(\mathbf{z}, \lambda_1, \lambda_2\right)}{\partial \left\|z_m\right\|_2^2} = -\frac{P_{k|k-1,m} R_{N,m} P_{k|k-1,m}}{\left(R_{N,m} + z_{k,m}^H z_{k,m} P_{k|k-1,m}\right)^2} + \lambda_1 L_{k,m,m} + \lambda_2, \tag{36}$$

with $L_{k,m,m}$ denoting the entry at mth row and mth column of $\mathbf{L}_k$. Therefore, we can obtain the optimized waveform $\mathbf{z}_k$ without the PAPR constraint as

$$\left\|z_{k,m}\right\|_2^2 = \max\left\{\sqrt{\frac{R_{N,m}}{\lambda_1 L_{k,m,m}+\lambda_2}} - \frac{R_{N,m}}{P_{k|k-1,m}}, 0\right\} \tag{37}$$

where λ_1 and λ_2 are used to control the detection performance and the transmitted power.

However, if the PAPR constraint is considered, $\mathbf{P}_{k|k-1}$ and $\mathbf{R}_N$ are no longer diagonal matrices. It is not easy to obtain an analytical expression for (31). Now we propose a novel method to solve this problem.

In the first step, we define $\mathbf{W}_k \triangleq \mathbf{s}_k\mathbf{s}_k^H$, where $\mathbf{W}$ is a real and symmetric matrix. Then we have

$$\begin{aligned}\mathbf{W}_k^* = \arg\min_{\mathbf{W}_k}\ & \mathrm{Tr}\left\{\left[\mathbf{P}_{k|k-1}^{-1} + \left(\mathbf{F}\mathbf{W}_k\mathbf{F}^H\right)^T \circ \mathbf{R}_N^{-1}\right]^{-1}\right\} \\ \text{s.t. } & \mathrm{Tr}\left\{\mathbf{W}_k\right\} = E_s \\ & \mathrm{Tr}\left\{\hat{\mathbf{G}}_k^H\mathbf{R}_N^{-1}\hat{\mathbf{G}}_k\mathbf{F}\mathbf{W}_k\mathbf{F}^H\right\} \geq \epsilon' \\ & \mathrm{diag}\left\{\mathbf{W}_k\right\} \leq \zeta' E_s.\end{aligned} \tag{38}$$

According to [2], the objective function $\mathrm{Tr}\left\{(\cdot)^{-1}\right\}$ is a convex function. Compared with (31), (38) relaxes the rank $\{\mathbf{W}\} = 1$ constraint, resulting in a convex optimization problem. Therefore, the CVX toolbox can be used to solve this problem [8], and we can then obtain the optimal real symmetric matrix $\mathbf{W}_k^*$.

In the second step, we must obtain the optimal waveform based on $\mathbf{W}_k^*$. If $\mathrm{rank}\left\{\mathbf{W}_k^*\right\} = 1$, then we have

$$\mathbf{W}_k^* = \mathbf{s}_k^*\mathbf{s}_k^{*H}, \tag{39}$$

where $\mathbf{s}_k^*$ is the optimum radar waveform in the time domain. If the rank $\left\{\mathbf{W}_k^*\right\} > 1$, then according to [10], we can use the eigenvector $\mathbf{c}_{\max}$ of $\mathbf{W}_k^*$ with the maximum eigenvalue acting as the reference signal. Then, the optimization problem can be represented as

$$\begin{aligned}\mathbf{s}_k^* = \arg\min_{\mathbf{s}_0}\ & \left\|\mathbf{s}_0 - \sqrt{E_s}\frac{\mathbf{c}_{\max}}{\|\mathbf{c}_{\max}\|_2}\right\|_2 \\ \text{s.t. } & \|\mathbf{s}_0\|_2^2 = E_s \\ & -\sqrt{\zeta' E_s} \leq \mathbf{s}_0 \leq \sqrt{\zeta' E_s} \\ & \mathbf{s}_0^H\left(\mathbf{F}^H\hat{\mathbf{G}}_k^H\mathbf{R}_N^{-1}\hat{\mathbf{G}}_k\mathbf{F}\right)\mathbf{s}_0 \geq \epsilon',\end{aligned} \tag{40}$$

where the objective function ensures that the optimized waveform $\mathbf{s}_k^*$ can well approach the direction of the eigenvector $\mathbf{c}_{\max}$. The three constraints, including the first con-

straint for the transmitted power, the second for the PAPR, and the third for the detection probability constraint, ensure that the optimal waveform satisfies the conditions considered in this work. Because the constraint $\mathbf{s}_0^H \left(\mathbf{F}^H \hat{\mathbf{G}}_k^H \mathbf{R}_N^{-1} \hat{\mathbf{G}}_k \mathbf{F}\right) \mathbf{s}_0 \geq \epsilon'$ in (40) is not a convex set, we must relax this constraint. Suppose $\mathbf{u}_{\max}$ is the eigenvector corresponding to the maximum eigenvalue $\theta_{\max}$ of $\mathbf{U} \triangleq \mathbf{F}^H \hat{\mathbf{G}}_k^H \mathbf{R}_N^{-1} \hat{\mathbf{G}}_k \mathbf{F}$. The detection constraint is

$$\mathbf{s}_0^H \operatorname{Re}\{\mathbf{u}_{\max}\} \geq \sqrt{\frac{\epsilon'}{\theta_{\max}}}. \tag{41}$$

According to the matrix eigenvalue decomposition,

$$\mathbf{U} = \sum_k \theta_k \mathbf{w}_k \mathbf{w}_k^H. \tag{42}$$

Because $\mathbf{U}$ is a semidefinite Hermitian matrix, then we can obtain that $\mathbf{s}_0^H \left(\mathbf{F}^H \hat{\mathbf{G}}_k^H \mathbf{R}_N^{-1} \hat{\mathbf{G}}_k \mathbf{F}\right) \mathbf{s}_0 \geq \epsilon'$ from (41). The optimization problem of (40) can then be written as a convex problem:

$$\begin{aligned} \mathbf{s}_k^* = \arg\min_{\mathbf{s}_0} & \left\| \mathbf{s}_0 - \sqrt{E_s} \frac{\mathbf{c}_{\max}}{\|\mathbf{c}_{\max}\|_2} \right\|_2 \\ \text{s.t. } & \|\mathbf{s}_0\|_2^2 = E_s \\ & -\sqrt{\zeta' E_s} \leq \mathbf{s}_0 \leq \sqrt{\zeta' E_s} \\ & \mathbf{s}_0^H \operatorname{Re}\{\mathbf{u}_{\max}\} \geq \sqrt{\frac{\epsilon'}{\theta_{\max}}}. \end{aligned} \tag{43}$$

The optimal radar waveform with rank $\left\{\mathbf{W}_k^*\right\} > 1$ can be obtained via the CVX toolbox.

4 Simulation Results

4.1 Transmitted Power Constraint

First, we give the estimation performance only with the constraint for the transmitted power. (38) can then be simplified as the following optimization problem (with the derivation details given in Appendix 2)

$$\begin{aligned} \mathbf{W}_k^* = \arg\min_{\mathbf{W}} & \operatorname{Tr}\left\{ \left[\mathbf{P}_{k|k-1}^{-1} + \left(\mathbf{F}\mathbf{W}\mathbf{F}^H\right)^T \circ \mathbf{R}_N^{-1} \right]^{-1} \right\} \\ \text{s.t. } & \operatorname{Tr}\{\mathbf{W}\} = E_s. \end{aligned} \tag{44}$$

If rank $\left\{\mathbf{W}_k^*\right\} = 1$, then the optimal radar signal $\mathbf{s}_0$ is

$$\mathbf{W}_k^* = \mathbf{s}_k^* \mathbf{s}_k^{*H}. \tag{45}$$

If rank $\left\{\mathbf{W}_k^*\right\} > 1$, then the optimal transmitted signal $\mathbf{s}_k^*$ is

$$\mathbf{s}_k^* = \sqrt{E_s} \frac{\mathbf{c}_{\max}}{\|\mathbf{c}_{\max}\|_2}. \tag{46}$$

The estimation performance of the optimal radar waveform based on (46) is compared with that of the random radar waveform. The simulation parameters are set as follows: the transmitted power is $E_s = 1$, the signal length is $L = 10$, the SNR of the echo signal is 7 dB, the temporal correlation constant is $\tau = 0.1$ṡ, and the PRI is $T = 1$ ms. To average the estimation performance, the number of random targets is set to be 50. The estimation performance is measured based on the normalized MSE, which is defined as

$$e_N \triangleq \mathcal{E}\left\{\frac{\|\hat{\mathbf{g}} - \mathbf{g}\|_2^2}{\|\mathbf{g}\|_2^2}\right\}, \tag{47}$$

where $\hat{\mathbf{g}}$ is the estimate of $\mathbf{g}$. For MAP estimation, we can obtain the expression for the normalized MSE with the specific waveform $\mathbf{s}_k$ as

$$e_N = \frac{1}{\|\mathbf{g}_k\|_2^2} \mathrm{Tr}\left\{\mathbf{Q}_k^H \mathbf{Q}_k \left(\mathbf{Z}_k \mathbf{g}_k \mathbf{g}_k^H \mathbf{Z}_k^H + \mathbf{R}_N\right) - \mathbf{g}_k^H \left(\mathbf{Z}_k^H \mathbf{Q}_k^H + \mathbf{Q}_k \mathbf{Z}_k - I\right) \mathbf{g}_k\right\}, \tag{48}$$

where $\mathbf{Z}_k = \mathrm{diag}\{\mathbf{F}\mathbf{s}_k\}$. For KF estimation at the kth iteration, the analytical expression for the normalized MSE of the waveform $\mathbf{s}_k$ is

$$e_N = \frac{1}{\|\mathbf{g}_k\|_2^2} \mathrm{diag}\left\{\mathbf{P}_{k|k-1} - \mathbf{\Phi}_k \mathbf{Q}_k \mathbf{Z}_k \mathbf{P}_{k|k-1}\right\}, \tag{49}$$

where the symbols are as defined in Algorithm 1 and $\mathbf{Z}_k = \mathrm{diag}\{\mathbf{F}\mathbf{s}_k\}$.

Figure 2 shows the normalized MSE of the estimated TSC, including the MAP and KF estimation methods. Because the KF can take advantage of the temporal TSC correlation, the performance of the KF estimation is better than that of the MAP method. Moreover, the performance can be further improved by optimizing the radar waveform via the proposed method.

4.2 Target Detection Probability Constraint

The feasibility of the waveform optimization method proposed in this work will be verified in the following. Without the PAPR constraint, we can obtain the optimized

radar waveform from (38) and (43) under the detection constraint. The optimization problem can then be rewritten as

$$\begin{aligned} \mathbf{W}_k^* = \arg\min_{\mathbf{W}} \ & \mathrm{Tr}\left\{\left[\mathbf{P}_{k|k-1}^{-1} + \left(\mathbf{F}\mathbf{W}\mathbf{F}^H\right)^T \circ \mathbf{R}_N^{-1}\right]^{-1}\right\} \\ \text{s.t. } & \mathrm{Tr}\{\mathbf{W}\} = E_s \\ & \mathrm{Tr}\left\{\hat{\mathbf{G}}_k^H \mathbf{R}_N^{-1} \hat{\mathbf{G}}_k \mathbf{F}\mathbf{W}\mathbf{F}^H\right\} \geq \epsilon'. \end{aligned} \tag{50}$$

The radar waveform from (43) can then be attained with some modifications as

$$\begin{aligned} \mathbf{s}_k^* = \arg\min_{\mathbf{s}_0} \ & \left\| \mathbf{s}_0 - \sqrt{E_s} \frac{\mathbf{c}_{\max}}{\|\mathbf{c}_{\max}\|_2} \right\|_2 \\ \text{s.t. } & \|\mathbf{s}_0\|_2^2 = E_s \\ & \mathbf{s}_0^H \,\mathrm{Re}\{\mathbf{u}_{\max}\} \geq \sqrt{\frac{\epsilon'}{\theta_{\max}}}. \end{aligned} \tag{51}$$

We first verify the constraint for detection probability during the waveform optimization. In the simulation, the false alarm probability is $P_{\mathrm{FA}} = 0.05$, the detection probability is $P_D \in [0.9, 0.99]$, and temporal correlation constants of the TSC during the radar pulse intervals are $\tau = 0.05\,\mathrm{s}$, $\tau = 0.1\,\mathrm{s}$, and $\tau = 0.15\,\mathrm{s}$. For the comparison, $\tau = \infty$ represents the unchanged TSC during the radar pulse interval. Figure 3 depicts the simulated target detection probability with different temporal correlation

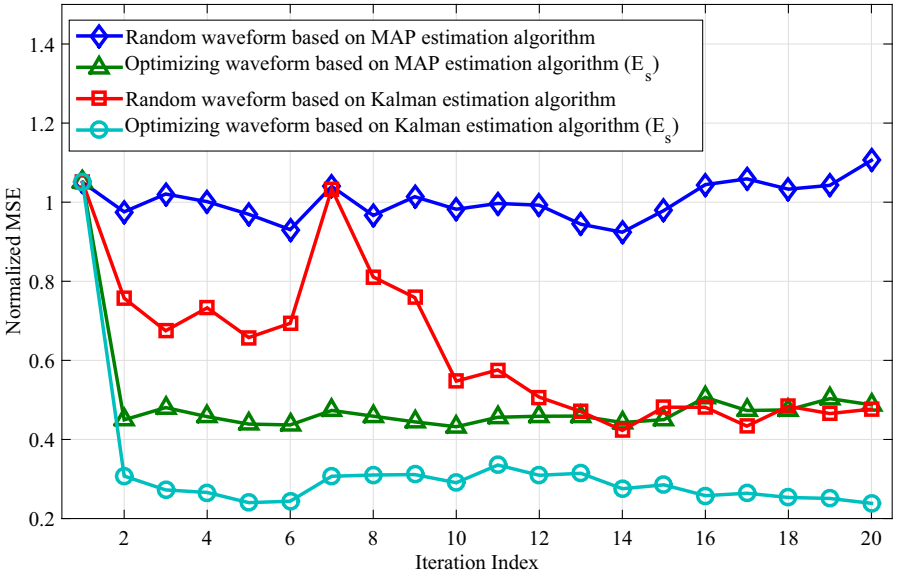

Fig. 2 Normalized MSE of the estimated TSC under the transmitted power constraint

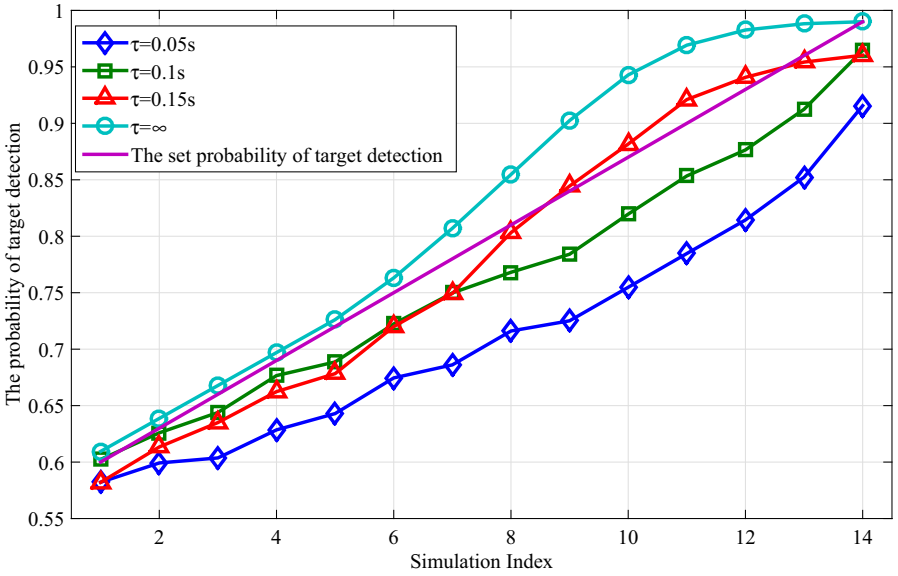

Fig. 3 Probability of target detection

constants and different constraints for detection probability. The figure shows that the simulated detection probability and the theoretical detection probability have a relatively high degree of agreement. Also, a larger TSC correlation between radar pulses leads to a higher degree of agreement. The difference between the simulated and theoretical target detection probabilities is mainly because the estimated TSC are based on the KF rather than the real TSC during radar waveform optimization. $\mathbf{s}_0^H \operatorname{Re}\{\mathbf{u}_{\max}\} \geq \sqrt{\frac{\epsilon'}{\theta_{\max}}}$ is used as a sufficient condition to satisfy the constraint of detection probability, which gives better performance than that using a prespecified constraint.

In the simulation, the PAPR is $< 3\,\text{dB}$, with the simulation results shown in Fig. 4. When the temporal correlation of TSC is sufficiently high, the simulated detection probability and the theoretical detection probability show a relatively high degree of agreement. However, the comparison with the simulated results shown in Fig. 3 without the PAPR constraint indicates that the PAPR constraint has little effect on the detection performance.

4.3 The PAPR Constraint

In this subsection, the simulated radar waveform optimization results under the transmitted power, PAPR and detection constraints are presented, where the temporal correlation constant is $\tau = 0.1\,\text{s}$. We set the PAPR constraint to be PAPR $\leq 3\,\text{dB}$. Then, we obtained the optimized waveform using the proposed method. To verify the feasibility of this PAPR constraint during waveform optimization, the differences between the PAPR of the optimized waveform and the PAPR constraint at each iteration are shown in Fig. 5, where the PAPR constraint of 3 dB is subtracted from the PAPR

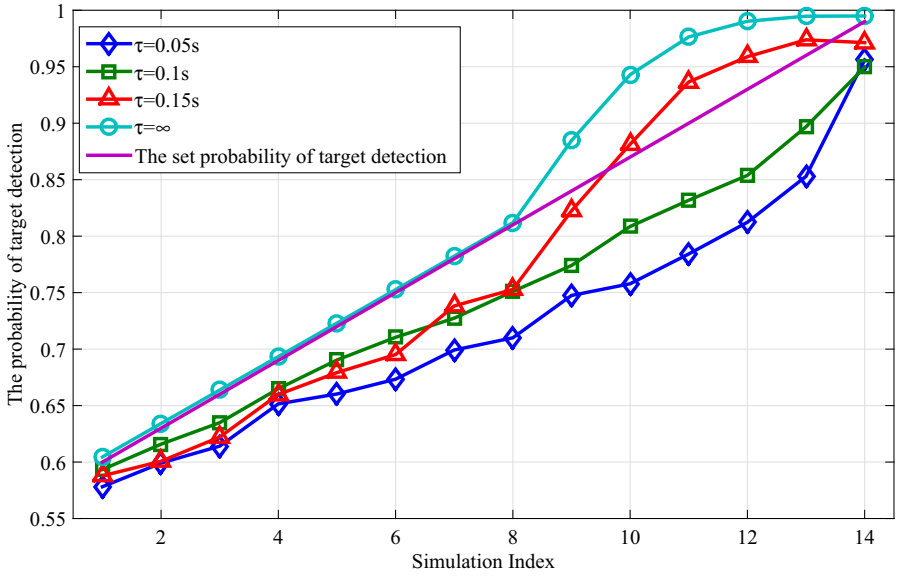

Fig. 4 Probability of target detection under the PAPR constraint

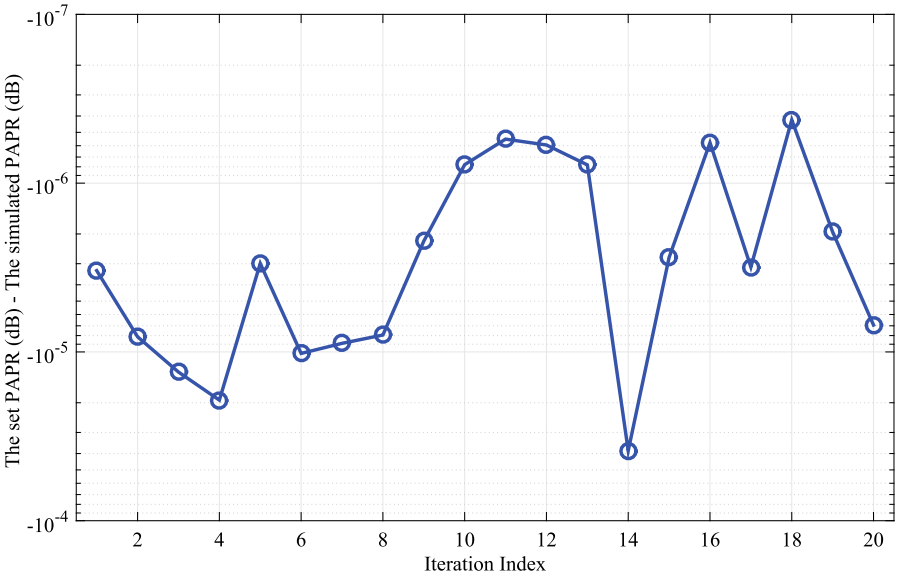

Fig. 5 Difference between simulated and set PAPR

of the optimized waveform. Because the results of subtraction during all iterations are positive, the PAPR of the optimized waveform must satisfy the preset PAPR constraint. However, the high agreement between the simulation and the PAPR constraint shows that the PAPR has a bad effect on the TSC estimation performance, but leads to high nonlinear power amplifier efficiency. Because the PAPR performance of the optimized

waveform is a constraint condition in the waveform design optimization problem proposed in this work, this performance cannot be improved by the optimization method. However, the optimized waveform does satisfy the PAPR constraint, which means that we can set the PAPR constraint before the waveform optimization process in the radar system. Then, an optimized waveform with a specific PAPR constraint can be obtained.

4.4 PAPR and Detection Constraints

Figure 6 depicts the estimation performance of the KF and MAP methods under the following constraints: PAPR$\leq$ 3 dB, $E_s = 1$, $P_{\mathrm{FA}} = 0.05$ and $P_D = 0.95$. The KF shows a better estimation performance than the MAP estimation method. Additionally, we compare the estimation performances of the optimized and random radar waveforms to verify the waveform optimization efficiency at each KF iteration step. Better estimation of the TSC can provide more information during radar waveform design so that target detection and target recognition can be better improved.

To compare the KF estimation performance under different constraints, Fig. 7 shows the simulation results for the waveform that was optimized using the method proposed in this paper under different constraints. The constraints are given as follows.

1. The E_s curve shows the KF estimation performance with the optimized waveform under two constraints as

$$\mathrm{Tr}\{\mathbf{W}\} = E_s \tag{52}$$

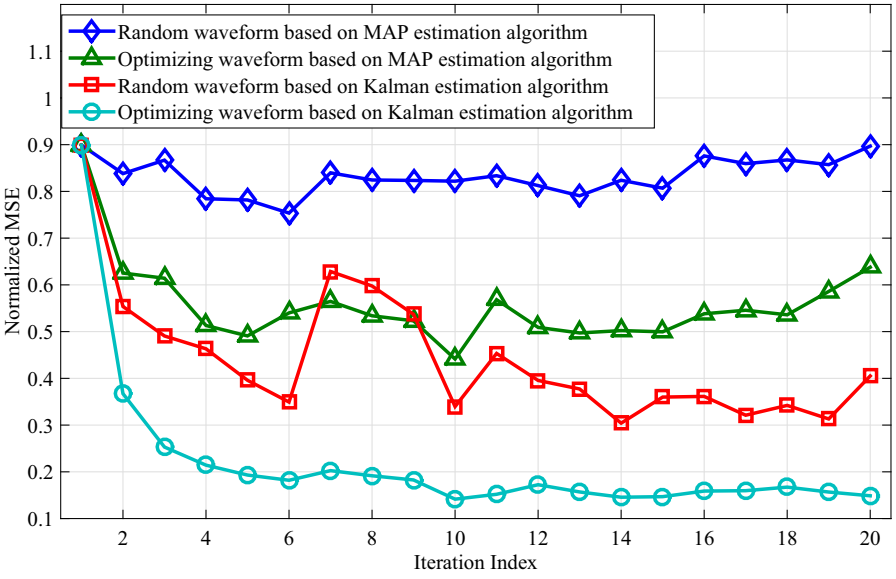

Fig. 6 Estimation performances of the different methods with different waveforms

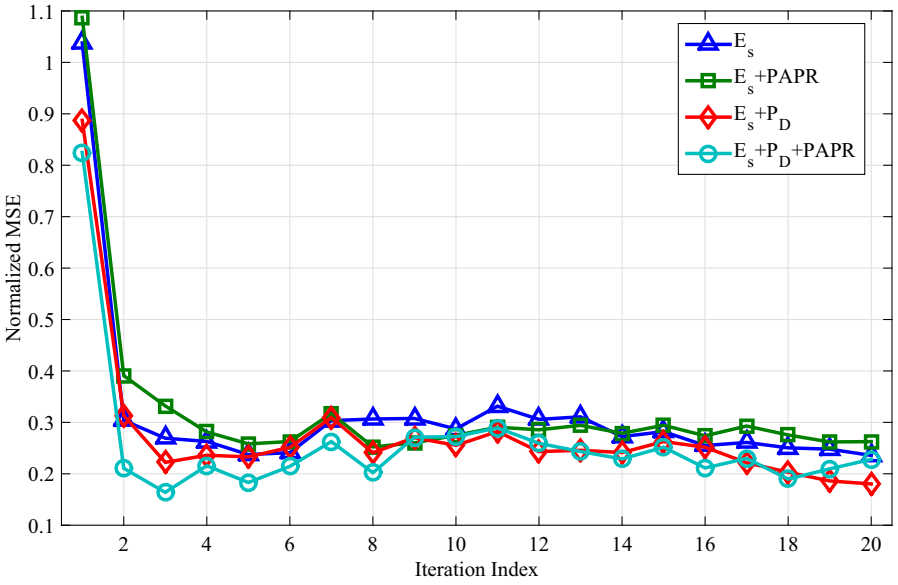

Fig. 7 Estimation performance of the KF method with the optimized waveform under the different constraints

in (38), and

$$\|\mathbf{s}_0\|_2^2 = E_s \tag{53}$$

in (43).

2. The E_s + PAPR curve shows the KF estimation performance with the optimized waveform under the following constraints as

$$\begin{aligned} &\mathrm{Tr}\{\mathbf{W}\} = E_s \\ &\mathrm{diag}\{\mathbf{W}\} \le \zeta' E_s \end{aligned} \tag{54}$$

in (38), and

$$\begin{aligned} &\|\mathbf{s}_0\|_2^2 = E_s \\ &-\sqrt{\zeta' E_s} \le \mathbf{s}_0 \le \sqrt{\zeta' E_s} \end{aligned} \tag{55}$$

in (43).

3. The $E_s + P_D$ curve shows the KF estimation performance with the optimized waveform under the following constraints as

$$\begin{aligned} &\mathrm{Tr}\{\mathbf{W}\} = E_s \\ &\mathrm{Tr}\left\{\hat{\mathbf{G}}_k^H \mathbf{R}_N^{-1} \hat{\mathbf{G}}_k \mathbf{F}\mathbf{W}\mathbf{F}^H\right\} \ge \epsilon' \end{aligned} \tag{56}$$

in (38), and

$$\|\mathbf{s}_0\|_2^2 = E_s \tag{57}$$
$$\mathbf{s}_0^H \,\mathrm{Re}\,\{\mathbf{u}_{\max}\} \geq \sqrt{\frac{\epsilon'}{\theta_{\max}}}$$

in (43).

4. The E_s + PAPR + P_D curve shows the KF estimation performance with the optimized waveform under the following constraints as

$$\mathrm{Tr}\,\{\mathbf{W}\} = E_s \tag{58}$$
$$\mathrm{Tr}\left\{\hat{\mathbf{G}}_k^H \mathbf{R}_N^{-1} \hat{\mathbf{G}}_k \mathbf{F}\mathbf{W}\mathbf{F}^H\right\} \geq \epsilon'$$
$$\mathrm{diag}\,\{\mathbf{W}\} \leq \zeta' E_s$$

in (38), and

$$\|\mathbf{s}_0\|_2^2 = E_s \tag{59}$$
$$-\sqrt{\zeta' E_s} \leq s_0 \leq \sqrt{\zeta' E_s}$$
$$\mathbf{s}_0^H \,\mathrm{Re}\,\{\mathbf{u}_{\max}\} \geq \sqrt{\frac{\epsilon'}{\theta_{\max}}}$$

in (43).

It can be seen from these simulation results that while the transmitted power, PAPR and detection constraints are used in the radar waveform design, there is no performance degradation with the introduction of the additional constraints for KF estimation with the optimized waveform.

5 Conclusions

In this work, novel TSC estimation and waveform design methods have been proposed for temporally correlated targets in CRS. By using the temporal correlation between pulses, the KF method has been used to estimate the TSC in the frequency domain. To minimize the MSE of the estimated TSC at each KF iteration, the radar waveform has been optimized by establishing an optimization problem under the constraints of transmitted power, PAPR and detection probability. Sine the original problem is non-convex, we have converted it into a convex one by rank relaxation. The simulation results show that the estimation performance is greatly improved by using the proposed method, and no performance degradation is observed with the introduction of the additional constraints for PAPR and detection probability. Future work will concentrate on waveform optimization for multiple extended targets, where different optimized waveforms can be obtained for different targets. A method must then be proposed to attain the transmitted waveform by trading off the optimized waveforms.

Acknowledgments This work was supported in part by the National Natural Science Foundation of China (Grant No.61271204 and No.61302097), by the National Key Technology R&D Program (Grant No.2012BAH12B00) and by the Ph.D. Programs Foundation of the Ministry of Education of China (Grant No.20120092120014).

Appendix 1: Derivation of the Objective Function

TSC estimation based on the MAP can be written as

$$\hat{\mathbf{g}}_k = \arg\max_{\mathbf{g}_k} \; p\left(\mathbf{g}_k | \, \mathbf{y}_k\right), \tag{60}$$

where the probability distribution of the TSC $\mathbf{g}_k$ given the echo waveform $\mathbf{y}_k$ can be written as

$$p\left(\mathbf{g}_k | \, \mathbf{y}_k\right) = \frac{p\left(\mathbf{g}_k, \mathbf{y}_k\right)}{p\left(\mathbf{y}_k\right)} = \frac{p\left(\mathbf{y}_k | \, \mathbf{g}_k\right) p\left(\mathbf{g}_k\right)}{p\left(\mathbf{y}_k\right)}. \tag{61}$$

The probability distribution of the echo waveform $\mathbf{y}_k$ given the TSC $\mathbf{g}_k$ is

$$p\left(\mathbf{y}_k | \, \mathbf{g}_k\right) = \frac{1}{(2\pi)^{\frac{M}{2}} \det\left(\mathbf{R}_N\right)^{\frac{1}{2}}} e^{-\frac{1}{2}\left(\mathbf{y}_k - \mathbf{Z}_k \mathbf{g}_\mathbf{k}\right)^H \mathbf{R}_N^{-1} \left(\mathbf{y}_k - \mathbf{Z}_k \mathbf{g}_\mathbf{k}\right)}. \tag{62}$$

The probability distribution of the TSC $\mathbf{g}_k$ is

$$p\left(\mathbf{g}_k\right) = \frac{1}{(2\pi)^{\frac{M}{2}} \det\left(\mathbf{R}_T\right)^{\frac{1}{2}}} e^{-\frac{1}{2}\mathbf{g}_k^H \mathbf{R}_T^{-1} \mathbf{g}_k}, \tag{63}$$

and the probability distribution of the echo waveform $\mathbf{y}_k$ is

$$p\left(\mathbf{y}_k\right) = \frac{1}{(2\pi)^{\frac{M}{2}} \det\left(\mathbf{R}_k\right)^{\frac{1}{2}}} e^{-\frac{1}{2}\mathbf{y}_k^H \mathbf{R}_k^{-1} \mathbf{y}_k}. \tag{64}$$

Then, we substitute (62), (63) and (64) into (61) and derive

$$\begin{aligned} p\left(\mathbf{g}_k | \, \mathbf{y}_k\right) &= \frac{p\left(\mathbf{y}_k | \, \mathbf{g}_k\right) p\left(\mathbf{g}_k\right)}{p\left(\mathbf{y}_k\right)} \\ &= \frac{e^{-\frac{1}{2}\left(\mathbf{y}_k - \mathbf{Z}_k \mathbf{g}_\mathbf{k}\right)^H \mathbf{R}_N^{-1} \left(\mathbf{y}_k - \mathbf{Z}_k \mathbf{g}_\mathbf{k}\right)} e^{-\frac{1}{2}\mathbf{g}_k^H \mathbf{R}_T^{-1} \mathbf{g}_k}}{(2\pi)^{\frac{M}{2}} \sqrt{\frac{\det\left(\mathbf{R}_T\right)\det\left(\mathbf{R}_N\right)}{\det\left(\mathbf{R}_k\right)}} e^{-\frac{1}{2}\mathbf{y}_k^H \mathbf{R}_k^{-1} \mathbf{y}_k}} \\ &= \frac{e^{-\frac{1}{2} f\left(\mathbf{g}_k\right)}}{(2\pi)^{\frac{M}{2}} \sqrt{\frac{\det\left(\mathbf{R}_T\right)\det\left(\mathbf{R}_N\right)}{\det\left(\mathbf{R}_k\right)}}}, \end{aligned} \tag{65}$$

where

$$f\left(\mathbf{g}_k\right) \triangleq \left(\mathbf{y}_k - \mathbf{Z}_k \mathbf{g}_k\right)^H \mathbf{R}_N^{-1} \left(\mathbf{y}_k - \mathbf{Z}_k \mathbf{g}_\mathbf{k}\right) + \mathbf{g}_k^H \mathbf{R}_T^{-1} \mathbf{g}_k - \mathbf{y}_k^H \mathbf{R}_k^{-1} \mathbf{y}_k \tag{66}$$

$$= \mathbf{y}_k^H \mathbf{R}_N^{-1} \mathbf{y}_k - \mathbf{g}_k^H \mathbf{Z}_k^H \mathbf{R}_N^{-1} \mathbf{y}_k - \mathbf{y}_k^H \mathbf{R}_N^{-1} \mathbf{Z}_k \mathbf{g_k} + \mathbf{g}_k^H \mathbf{Z}_k^H \mathbf{R}_N^{-1} \mathbf{Z}_k \mathbf{g_k} + \mathbf{g}_k^H \mathbf{R}_T^{-1} \mathbf{g}_k - \mathbf{y}_k^H \mathbf{R}_k^{-1} \mathbf{y}_k.$$

Therefore, the TSC $\mathbf{g}_k$ that can maximize the posteriori probability $p(\mathbf{g}_k | \mathbf{y}_k)$ can also minimize $f(\mathbf{g}_k)$. (60) can then be simplified as

$$\begin{aligned}
\hat{\mathbf{g}}_k &= \arg\max_{\mathbf{g}_k} \; p(\mathbf{g}_k | \mathbf{y}_k) \\
&= \arg\min_{\mathbf{g}_k} \; f(\mathbf{g}_k) \\
&= \arg\min_{\mathbf{g}_k} \; \mathbf{y}_k^H \mathbf{R}_N^{-1} \mathbf{y}_k - \mathbf{g}_k^H \mathbf{Z}_k^H \mathbf{R}_N^{-1} \mathbf{y}_k - \mathbf{y}_k^H \mathbf{R}_N^{-1} \mathbf{Z}_k \mathbf{g_k} \\
&\quad + \mathbf{g}_k^H \mathbf{Z}_k^H \mathbf{R}_N^{-1} \mathbf{Z}_k \mathbf{g_k} + \mathbf{g}_k^H \mathbf{R}_T^{-1} \mathbf{g}_k - \mathbf{y}_k^H \mathbf{R}_k^{-1} \mathbf{y}_k \\
&= \arg\min_{\mathbf{g}_k} \; \mathbf{g}_k^H \left(\mathbf{Z}_k^H \mathbf{R}_N^{-1} \mathbf{Z}_k + \mathbf{R}_T^{-1} \right) \mathbf{g}_k - \mathbf{y}_k^H \mathbf{R}_N^{-1} \mathbf{Z}_k \mathbf{g}_k - \mathbf{g}_k^H \mathbf{Z}_k^H \mathbf{R}_N^{-1} \mathbf{y}_k,
\end{aligned} \tag{67}$$

which is (7).

Appendix 2: Simplification of the Optimization Problem

First, we present the derivation of (38). In (31), the objective function is

$$\begin{aligned}
\mathbf{z}_k^* &= \arg\min_{\mathbf{z}_k} \; \mathrm{Tr}\left\{ \left(\mathbf{P}_{k|k}^{-1} + \mathbf{V}_k \circ \mathbf{R}_N^{-1} \right)^{-1} \right\} \left(\text{where } \mathbf{V}_k \triangleq \left(\mathbf{z}_k \mathbf{z}_k^H \right)^T \right) \\
&= \arg\min_{\mathbf{z}_k} \; \mathrm{Tr}\left\{ \left(\mathbf{P}_{k|k}^{-1} + \left(\mathbf{z}_k \mathbf{z}_k^H \right)^T \circ \mathbf{R}_N^{-1} \right)^{-1} \right\}.
\end{aligned} \tag{68}$$

Then, by using the Fourier transform $\mathbf{z}_k = \mathbf{F}\mathbf{s}_k$, this objective function can be rewritten in time domain as:

$$\mathbf{s}_k^* = \arg\min_{\mathbf{s}_k} \; \mathrm{Tr}\left\{ \left(\mathbf{P}_{k|k}^{-1} + \left(\mathbf{F}\mathbf{s}_k \mathbf{s}_k^H \mathbf{F}^H \right)^T \circ \mathbf{R}_N^{-1} \right)^{-1} \right\}. \tag{69}$$

In (38), we define $\mathbf{W}_k \triangleq \mathbf{s}_k \mathbf{s}_k^H$. Then the objective function to attain the optimal waveform matrix $\mathbf{W}_k$ is

$$\mathbf{W}_k^* = \arg\min_{\mathbf{W}_k} \; \mathrm{Tr}\left\{ \left[\mathbf{P}_{k|k-1}^{-1} + \left(\mathbf{F}\mathbf{W}_k \mathbf{F}^H \right)^T \circ \mathbf{R}_N^{-1} \right]^{-1} \right\}. \tag{70}$$

The constraints in (38) can be represented by the waveform matrix $\mathbf{W}_k$. The first power constraint is equivalent to

$$\mathrm{Tr}\{\mathbf{W}_k\} = \mathbf{s}_k^H \mathbf{s}_k = E_s. \tag{71}$$

The second target detection constraint is

$$p(\mathbf{z}_k) = \mathbf{z}_k^H \hat{\mathbf{G}}_k^H \mathbf{R}_N^{-1} \hat{\mathbf{G}}_k \mathbf{z}_k' \tag{72}$$

$$= \mathrm{Tr}\left\{\mathbf{z}_k^H \hat{\mathbf{G}}_k^H \mathbf{R}_N^{-1} \hat{\mathbf{G}}_k \mathbf{z}_k\right\}$$
$$= \mathrm{Tr}\left\{\hat{\mathbf{G}}_k^H \mathbf{R}_N^{-1} \hat{\mathbf{G}}_k \mathbf{F}\mathbf{W}_k\mathbf{F}^H\right\} \geq \epsilon'.$$

And the third PAPR constraint can be written as

$$\mathrm{diag}\{\mathbf{W}_k\} \leq \zeta' E_s. \tag{73}$$

Therefore, by combining the objective function (70) with the three constraints (71), (72) and (73), we derive the optimization problem and obtain the optimized waveform matrix $\mathbf{W}_k^*$ as

$$\begin{aligned} \mathbf{W}_k^* = \arg\min_{\mathbf{W}_k} \ & \mathrm{Tr}\left\{\left[\mathbf{P}_{k|k-1}^{-1} + \left(\mathbf{F}\mathbf{W}_k\mathbf{F}^H\right)^T \circ \mathbf{R}_N^{-1}\right]^{-1}\right\} \\ \text{s.t. } & \mathrm{Tr}\{\mathbf{W}_k\} = E_s \\ & \mathrm{Tr}\left\{\hat{\mathbf{G}}_k^H \mathbf{R}_N^{-1} \hat{\mathbf{G}}_k \mathbf{F}\mathbf{W}_k\mathbf{F}^H\right\} \geq \epsilon' \\ & \mathrm{diag}\{\mathbf{W}_k\} \leq \zeta' E_s, \end{aligned} \tag{74}$$

which is (38).

Second, if we only consider the transmitted power constraint, (74) reduces to

$$\begin{aligned} \mathbf{W}_k^* = \arg\min_{\mathbf{W}} \ & \mathrm{Tr}\left\{\left[\mathbf{P}_{k|k-1}^{-1} + \left(\mathbf{F}\mathbf{W}\mathbf{F}^H\right)^T \circ \mathbf{R}_N^{-1}\right]^{-1}\right\} \\ \text{s.t. } & \mathrm{Tr}\{\mathbf{W}\} = E_s, \end{aligned} \tag{75}$$

which is (44). If we add the target detection constraint, we can obtain the optimization problem in (50).

References

1. M. Bell, Information theory and radar waveform design. IEEE Trans. Inf. Theory **39**(5), 1578–1597 (1993)
2. S. Boyd, L. Vandenberghe, *Convex Optimization* (Cambridge University Press, Cambridge, 2004)
3. F. Dai, *Wideband Radar Signal Processing*. Doctoral thesis, Xidian University, 2010
4. F. Dai, H. Liu, P. Wang, S. Xia, Adaptive waveform design for range-spread target tracking. Electron. Lett. **46**(11), 793–794 (2010)
5. X. Deng, C. Qiu, Z. Cao, M. Morelande, B. Moran, Waveform design for enhanced detection of extended target in signal-dependent interference. IET Radar Sonar Navig. **6**(1), 30–38 (2012)
6. M. Fan, D. Liao, X. Ding, X. Li, Waveform design for target recognition on the background of clutter. *In 2011 European Radar Conference* Manchester, 329–332 2011
7. X. Gong, H. Meng, Y. Wei, X. Wang, Phase-modulated waveform design for extended target detection in the presence of clutter. Sensors **11**(7), 7162–7177 (2011)
8. M. Grant, S. Boyd, CVX: matlab software for disciplined Convex programming, version 2.1. http://cvxr.com/cvx (2014). Accessed 7 June 2014
9. S. Haykin, Cognitive radar: a way of the future. IEEE Signal Process. Mag. **23**, 30–40 (2006)

10. Z. Luo, W. Ma, A.M. So, Y. Ye, S. Zhang, Semidefinite relaxation of quadratic optimization problems. IEEE Signal Process. Mag. **27**(3), 20–34 (2010)
11. H.D. Meng, Y.M. Wei, X.H. Gong, Y.M. Liu, X.Q. Wang, Radar waveform design for extended target recognition under detection constraints. Math. Probl. Eng. **2012**(2012), 1–15 (2012)
12. R. Mohseni, A. Sheikhi, M.A. Masnadi Shirazi, Constant envelope OFDM signals for radar applications. *In Proceedings IEEE Radar Conference*, Rome, 1–5 2008
13. R. Mohseni, A. Sheikhi, M.A. Masnadi-Shirazi, Multicarrier constant envelope OFDM signal design for radar applications. Aeu-Int. J. Electron. Commun. **64**(11), 999–1008 (2010)
14. L.K. Patton, B.D. Rigling, Autocorrelation and modulus constraints in radar waveform optimization. *In Proceedings International Waveform Diversity Design Conference*, Kissimmee, FL, 150–154 2009
15. L. Patton, S. Frost, B. Rigling, Efficient design of radar waveforms for optimised detection in coloured noise. IET Radar Sonar Navig. **6**(1), 21 (2012)
16. R. Romero, N. Goodman, Waveform design in signal-dependent interference and application to target recognition with multiple transmissions. IET Radar Sonar Navig. **3**(4), 328 (2009)
17. S. Sen, Adaptive OFDM Radar for Target Detection and Tracking. doctoral thesis, Washington University in St. Louis, 2010
18. S. Sen, Constant-envelope waveform design for optimal target-detection and autocorrelation performances. *In Proceedings ICASSP*, Vancouver, BC, 3851–3855 2013
19. S. Sen, C. Glover, Optimal multicarrier phase-coded waveform design for detection of extended targets. *In Proceedings Radar Conference*, Ottawa, ON, 1–6 2013
20. S. Sen, A. Nehorai, OFDM MIMO radar design for low-angle tracking using mutual information. *In 3rd IEEE Int. Work. Comput. Adv. Multi-Sensor Adapt. Process.*, Aruba, Dutch Antilles, 173–176 2009
21. S. Sen, A. Nehorai, OFDM MIMO radar with mutual-information waveform design for low-grazing angle tracking **58**(6), 3152–3162 (2010)
22. S. Sen, Characterizations of PAPR-constrained radar waveforms for optimal target detection. IEEE Sens. J. **14**(5), 1647–1654 (2014)
23. S. Sen, PAPR-constrained pareto-optimal waveform design for OFDM-STAP radar. IEEE Trans. Geosci. Remote Sens. **52**(6), 3658–3669 (2014)
24. S.C. Thompson, J.P. Stralka, Constant envelope OFDM for power-efficient radar and data communications. *In: Proc. Int. Waveform Divers. Des. Conf.*, Kissimmee, FL, 291–295 2009
25. B. Wang, W.F. Yang, J.K. Wang, Adaptive waveform design for multiple radar tasks based on constant modulus constraint. J. Appl. Math., 1–6 (2013)
26. Y. Wei, H. Meng, Y. Liu, X. Wang, Radar phase-coded waveform design for extended target recognition under detection constraints. I*n Radar Conf.*, Kansas City, MO, 1074–1079 2011
27. F. Weinmann, Frequency dependent RCS of a generic airborne target. *In Proc. URSI Int. Symp. Electromagn. Theory*, Berlin, Germany 977–980 2010
28. Y. Yang, R. Blum, MIMO radar waveform design based on mutual information and minimum mean-square error estimation. IEEE Trans. Aerosp. Electron. Syst. **43**(1), 330–343 (2007)
29. X. Zhang, C. Cui, Range-spread target detecting for cognitive radar based on track-before-detect. Int. J. Electron. **101**(1), 74–87 (2014)